Zwitterionic polymer-coated ultrasmall superparamagnetic iron oxide nanoparticles with low protein interaction and high biocompatibility

Pombo-García, K.; Weiss, S.; Zarschler, K.; Ang, C.-S.; Hübner, R.; Pufe, J.; Meister, S.; Seidel, J.; Pietzsch, J.; Spiccia, L.; Stephan, H.; Graham, B.;

Originally published:

September 2016

ChemNanoMat 2(2016)10, 959-971

DOI: https://doi.org/10.1002/cnma.201600233

Zwitterionic polymer-coated ultrasmall superparamagnetic iron oxide nanoparticles with low protein interaction and high biocompatibility

Karina Pombo-García,[a] Stephan Weiss,[b] Kristof Zarschler,[a] Ching-Seng Ang,[c] René Hübner,[d] Johanna Pufe,[a] Sebastian Meister,[a] Jürgen Seidel,[e] Jens Pietzsch,[a,f] Leone Spiccia,*[g] Holger Stephan,*[a] and Bim Graham*[h]

Abstract: We report the synthesis and detailed *in vitro* evaluation of zwitterionic ultrasmall superparamagnetic iron oxide NPs (USPIONs) comprised of oleic acid/oleyl alcohol-stabilized magnetite particles (5 nm core diameter) coated with an amphiphilic zwitterionic polymer, poly(maleic anhydride-alt-1-decene) substituted with 3-(dimethylamino)propylamine (PMAL). These particles display a near-neutral zeta potential at pH ≥ 7 and possess high colloidal stability, maintaining a hydrodynamic diameter of *ca.* 15–20 nm over a wide range of pHs (4–10) and ionic strength (up to 1 M NaCl). They exhibit very low levels of nonspecific protein binding upon exposure to serum, and negligible uptake by phagocytic and non-phagocytic hepatocarcinoma cells, which suggests that they may be able to resist rapid accumulation in the liver and spleen, a common *in vivo* fate for NPs. The PMAL-USPIONs exhibit very low cytotoxicity and do not elicit an inflammatory response or display hemolytic activity *in vitro*. Minimal nonspecific uptake by either cancerous or non-cancerous cell lines was observed, an important precondition to achieve highly selective targeting upon further functionalization with an active targeting agent (*e.g.*, antibody or peptide). Overall, this study establishes the considerable potential of PMAL-USPIONs as a platform for the future development of “stealth” NP-based imaging and/or therapeutic agents.

[a] Dr. K. Pombo-Garcia, Dr. K. Zarschler, J. Pufe, S. Meister, Prof. J. Pietzsch, Dr. H. Stephan
Institute of Radiopharmaceutical Cancer Research
Helmholtz-Zentrum Dresden-Rossendorf
D 01328 Dresden, Germany
Email: h.stephan@hzdr.de
[b] S. Weiss
Institute of Resource Ecology
Helmholtz-Zentrum Dresden-Rossendorf
D 01328 Dresden, Germany
[c] Dr. C.-S. Ang
Bio21 Molecular Science and Biotechnology Institute
The University of Melbourne
Melbourne, VIC 3010, Australia
[d] Dr. R. Hübner
Institute of Ion Beam Physics and Material Research
Helmholtz-Zentrum Dresden-Rossendorf
D 01328 Dresden, Germany
[e] Dr. J. Seidel
Institute of Physical Chemistry
Technische Universität Bergakademie Freiberg
D 09596 Freiberg, Germany
[f] Department of Chemistry and Food Chemistry
Technische Universität Dresden
D 01062 Dresden, Germany
[g] Prof. L. Spiccia
School of Chemistry
Monash University
Clayton, VIC 3800, Australia
Email: leone.spiccia@monash.edu
[h] Assoc. Prof. B. Graham
Monash Insitute of Pharmaceutical Sciences
Monash University
Parkville, VIC 3052, Australia
Email: bim.graham@monash.edu

Supporting information for this article is given via a link at the end of the document.

Introduction

Magnetic iron oxide nanoparticles (NPs) are (potentially) useful for a broad range of applications, ranging from drug delivery, medical imaging and therapy.[1] Below a certain size, these NPs behave as superparamagnets, which can be exploited for hyperthermia treatment of tumors, and in magnetic resonance imaging (MRI), a powerful non-invasive medical imaging technique providing excellent tissue contrast and detailed anatomical information.[2] As for other NPs, however, the clinical application of ultrasmall superparamagnetic iron oxide NPs (USPIONs) is currently hampered by a lack of detailed understanding and control over their fate *in vivo*.

In addition to size and shape, the surface properties of NPs have a tremendous effect on their *in vitro* and *in vivo* behaviour,[3-6] including biodistribution,[7] toxicity,[8] cellular immune response[9] and clearance.[10] The exposure of most NPs to proteins or complex biological environments triggers the nonspecific adsorption of biomolecules to their surface.[11-13] Biomolecular corona formation results in opsonization as well as scavenging of NPs by the mononuclear phagocyte system (MPS; also referred to as the reticuloendothelial system, or RES), leading to eventual accumulation in the liver and spleen.[14, 15] As a consequence, there continues to be strong interest in the development of surface functionalization strategies that not only render NPs water-dispersible and colloidally stable, but also provide them with anti-fouling properties and good overall biocompatability.[16]

One of the most widely employed procedures involves attachment of polymeric ethoxyethylene units (PEGylation).[17, 18] These highly hydrophilic polymers make biomolecule adsorption thermodynamically unfavorable.[4, 19] However, PEGylation can significantly increase the effective hydrodynamic diameter (HD) of NPs, which prevents their flow into confined spaces and impedes their renal elimination *in vivo*.[10, 20] The majority of

PEGylated particles therefore still up end in MPS organs, which hampers their clinical translation.[21]

Zwitterionic ligands that contain both positively and negatively charged groups represent attractive alternatives for the functionalization of NP surfaces, since these substances can provide water dispersibility and high colloidal stability over a wide range of pH and ionic strength, as well as reduce the nonspecific interaction of NPs with serum proteins, without necessarily contributing greatly to the overall HD.[3, 20, 22] [23-26] By way of example, Bawendi and coworkers have reported that the coating of USPIONs with zwitterionic dopamine sulfonate ligands provides very stable, narrow-sized (10 nm) NPs for *in vitro* and *in vivo* imaging applications,[27] [2] Mondini *et al*.[28] reported that zwitterionic dopamine sulfonate-stabilized iron oxide NPs are superior to their PEGylated counterparts with respect to stability and show negligible interaction with proteins *in vitro*. Likewise, monodisperse, colloidally stable USPIONs (< 6 nm) featuring a zwitterionic coating formed from a sulfobetaine siloxane derivative are capable of avoiding protein corona formation.[29] Sulfobetaine-coated USPIONs have also been obtained *via* hydrophobic interaction of oleic acid-stabilized NPs with sulfobetaine derivatives incorporating long alkyl chains, producing NPs suitable for tumor and lymph node imaging in mice.[30]

In addition to these (and other) low-molecular weight zwitterionic coating materials, a number of zwitterionic polymers have also been employed in the development of water-dispersible NPs for potential biomedical applications, including poly(carboxybetaine)[29] and poly(sulfobetaine) derivatives,[31] phosphorylcholine-based copolymers,[32] and poly(acrylic) acid[33] and poly(maleic anhydride-alt-1-alkene) derivatives.[34] Compared to low molecular weight compounds that are anchored to a NP surface by only or two groups, polymers containing multiple anchoring groups can generate significantly more stable coatings, leading to enhanced colloidal stability across a wider range of conditions. For the most part, zwitterionic polymers have been applied to the stabilization of quantum dots and gold NPs,[35-40] although, for example, Xiao *et al.*[33] have reported the zwitterionic modification of iron oxide NPs through conjugation of 3-(diethylamino)propylamine to poly(acrylic acid)-coated magnetite NPs, leading to prolonged *in vivo* circulation time.

As part of a program directed towards the production of new multi-modal imaging agents, we recently described the preparation of USPIONs coated with octylamine-modified polyacrylic acid (OPA-USPIONs).[41] Although these hydrophilic NPs proved to be highly colloidal stable in aqueous solution, exposure to serum led to rapid protein corona formation, suggesting they would likely be scavenged *in vivo* by the MPS. We now report that replacement of the negatively charged OPA polymer in this earlier design with a zwitterionic analog, poly(maleic anhydride-alt-1-decene) modified with 3-(dimethylamino)propylamine (PMAL), produces water-dispersible USPIONs with considerably enhanced "stealth" properties. In addition to presenting the synthesis and detailed physico-chemical characterization of the new PMAL-USPIONs, we describe the results of a detailed study examining the colloidal stability of the NPs under a range of conditions (including in serum), their interaction with serum proteins, their cytocompatibility, hemolytic activity and inflammation-inducing capacity.

Results and Discussion

2.1 Synthesis and physico-chemical characterization

Oleic acid/oleyl alcohol-stabilized magnetite USPIONs with a core diameter of *ca.* 5 nm were prepared as described earlier.[42] These were coated with the commercially available amphiphilic polymer PMAL-C8 (poly(maleic anhydride-alt-1-decene) modified with 3-(dimethylamino)propylamine, M_w = 18.5 kDa) [43] by incubating the NPs with an excess of the polymer in chloroform for 1 h, followed by evaporation of the solvent, suspension in water and removal of excess PMAL and NP aggregates by ultracentrifugation and ultrafiltration. During this process, the octyl chains of the PMAL intercalate between the hydrocarbon tails of the oleic acid and oleyl alcohol *via* hydrophobic interactions, leading to the formation of stable and water-soluble organic-inorganic hybrid NPs denoted as PMAL-USPIONs. The outer layer of these particles features an even distribution of tertiary amine and carboxylic acid groups which are attached to the PMAL polymer, resulting in an overall zwitterionic surface (Figure 1).

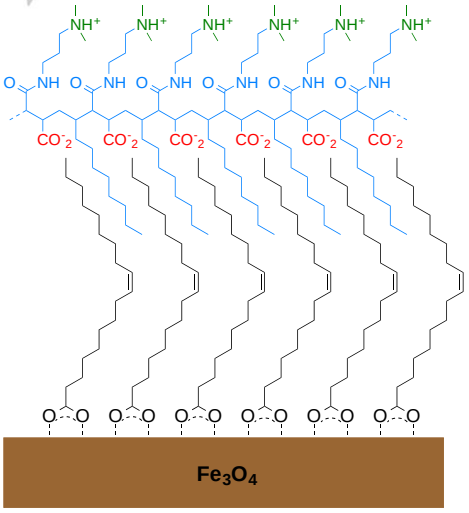

Figure 1. Representation of the surface of the PMAL-USPIONs. The PMAL polymer is shown in blue, with the charged groups highlighted. Note that the surface also contains a fraction of oleyl alcohol molecules, which are not shown.

Transmission electron microscopy (TEM) showed that the PMAL-USPIONs were monodisperse (Figure S1) and high-resolution TEM (HRTEM) revealed a *ca.* 5 nm-diameter crystalline magnetite core with a PMAL shell of *ca.* 1 nm thickness (Figure 2A). The crystal structure of the magnetite

core was confirmed by powder XRD (Figure 2B) and a crystallite size of 5.1 nm was calculated from the (311) peak *via* the Debye-Scherrer equation,[44] which is consistent with the HRTEM results. Dynamic light scattering (DLS) analysis (Figure 2C) revealed that coating with PMAL increases the hydrodynamic diameter (HD) to 15 nm, with the size distribution remaining monodisperse. The increase in HD is attributable to the physical size of the polymer and its strong interaction with surrounding water molecules.[45]

A number of methods were used to quantify the amount of PMAL and number of surface carboxylic acid groups within the PMAL-USPIONs, with the results summarized in Table 1. Thermogravimetric analysis (TGA) of the PMAL-USPIONs (Figure 2D) showed a mass loss of *ca.* 5% at temperatures < 200°C, corresponding to loss of water, followed by a 40% mass loss attributable to degradation of organic material (PMAL, oleic acid and oleyl alcohol) over a temperature range from 200 to 600°C; the remaining non-combusted mass (55%) corresponds to pure magnetite. In contrast, the oleic acid/oleyl alcohol-stabilized USPIONs showed a mass loss of *ca.* 30% over the same temperature range. This indicates that the PMAL accounts for *ca.* 10% of the mass of the PMAL-USPIONs. Based on this, the number of carboxylic groups per single PMAL-USPION was estimated to be *ca.* 100 (see Section 2 of ESI for details). Elemental (combustion) analysis of the purified PMAL-USPIONs showed that they contain 0.73 ± 0.1% nitrogen by mass, which also indicates that *ca.* 10% of the total mass is made up of polymer (the only N-containing component of the coated NPs, comprised of 8% N by mass). Based on the TGA result that 55% of the mass of the PMAL-USPIONS is magnetite, we again estimate *ca.* 100 COOH groups per NP (see section 2 of ESI for details). Finally, a potentiometric titration analysis was performed in order to directly measure the number of COOH groups on the surface. The number of carboxylic groups was calculated by fitting a thermodynamically based charge-balance equation, [46, 47] considering two different protonable sites (tertiary amine and carboxylate groups) to the experimental pH-titration data. A value of *ca.* 150 COOH groups was obtained.

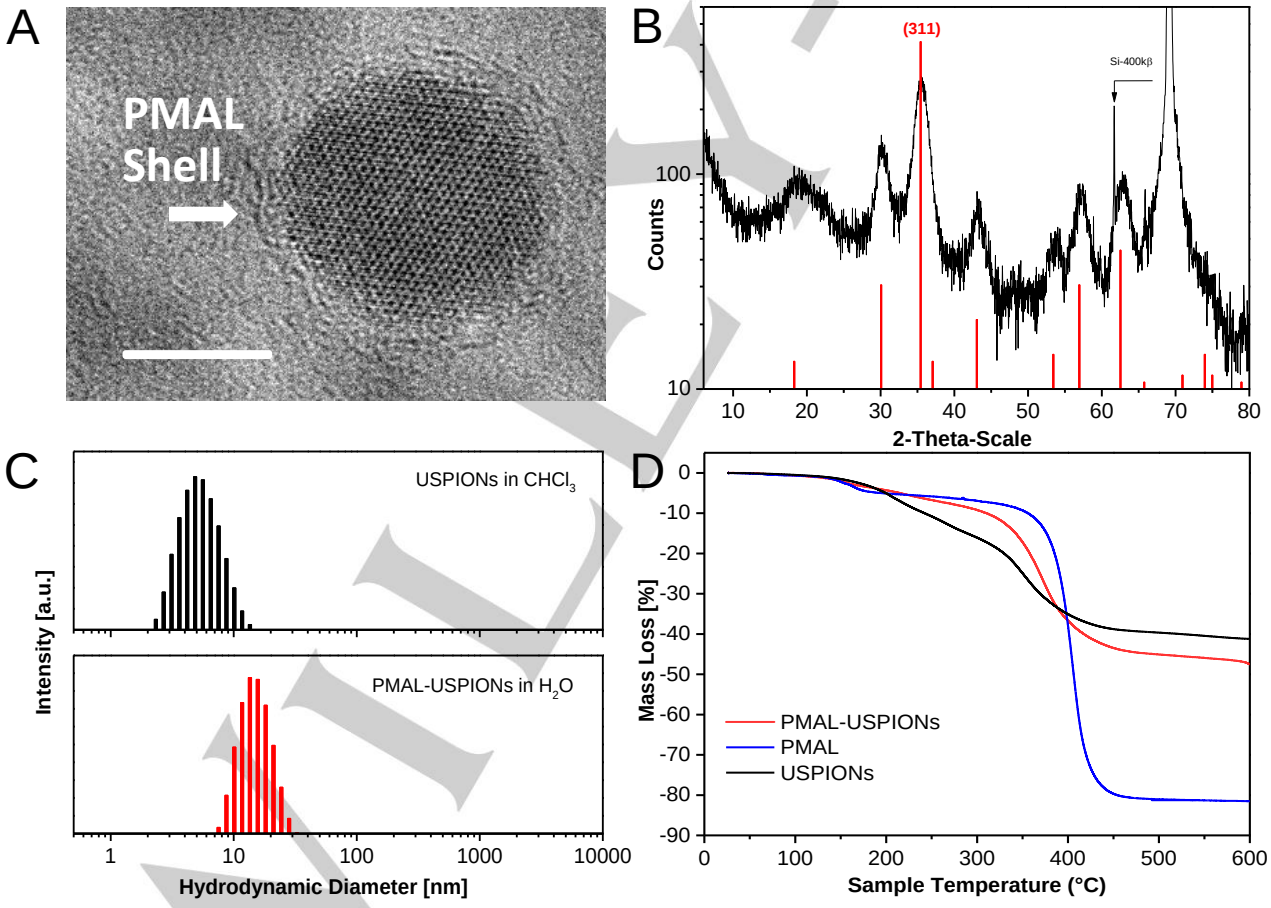

Figure 2. Physico-chemical characterization of the USPIONs. (A) HRTEM micrograph of a single magnetite nanoparticle coated with PMAL (scale bar = 5 nm). (B) XRD pattern of PMAL-USPIONs powder, together with the diffraction pattern of magnetite (PDF 04-007-2718, red bars). (C) DLS particle size distributions for oleic acid/oleyl alcohol-stabilized USPIONs (polydispersity index, PdI = 0.134) and purified PMAL-USPIONs (PdI = 0.26). (D) TGA of PMAL-USPIONs, oleic acid/oleyl alcohol-stabilized USPIONs and PMAL.

Table 1. PMAL content and surface concentration of carboxylic acid groups for PMAL-USPIONs.

Method	PMAL content (% of total mass)	No. COOH groups per particle	No. COOH groups per nm^2 [a]
TGA	10 ± 3	109 ± 27	1.4 ± 0.4
Elemental analysis	9 ± 2	100 ± 25	1.3 ± 0.3
Titration	-	155 ± 18	2.0 ± 0.3

[a] Expressed relative to the surface area of the magnetite core.

2.2. Colloidal stability

Given that colloidal stability is one of the most important issues for the final biological application of NPs, the stability of the PMAL-USPIONs was examined. Figure 3 shows the zeta potential and HD of the PMAL-USPIONs, measured over the pH range 4–10. The zeta potential is determined by protonation/deprotonation of the carboxylic groups (pK_a ~ 5–6)[48] and tertiary amines (pK_a ≥ 10)[49] present in the PMAL coating. Consistent with the pK_a values of these groups, the overall surface charge of the NPs was found to be close to neutral in the pH 7–10 range (the species distribution calculated from the fitting of the potentiometric data indicated that at pH 7 all of the amino groups are protonated and > 80% of the carboxylic groups are deprotonated). The zeta potential became progressively more positive as the pH decreased from 7, due to gradual protonation of the carboxylate groups, reaching a value of *ca.* 17 mV at pH 4 (Figure 3A) (note that polymers incorporating, for example, quaternary amine and sulfonate groups could potentially be employed to extend the pH range over which the surface remains neutral, but these are not yet commercially available). The HD of the NPs varied very little with pH, remaining at around 15–20 nm and remained stable for over a month when the NPs were kept at pH ≤ 7 (Figure 3B). Long-term stability was limited at lower pH. The high stability of the PMAL-USPIONs, especially under conditions where the zeta potential is close to 0 mV, raises the possibility of steric stabilization, where polymers on the surface prevent convergence of the magnetite cores and NP aggregation promoted by Van der Waals forces. Electrostatic stabilization can be ruled out, at least for pH values above 7.

An evaluation of the stability at different ionic strengths (10 mM to 1 M NaCl) revealed no significant change in HD (Figure S3) or evidence of precipitation. The PMAL-USIONs also proved to be stable in biologically relevant solutions, such as serum-free cell culture media (DMEM), fetal bovine serum-containing cell culture media (DMEM + 10% FBS) and phosphate-buffered saline (PBS 1X), with the HD remaining at *ca.* 15 nm (Figure 3B). No change in HD was observed after six month's storage in 50 mM phosphate buffer (pH 7.4) (Figure S3). The high stability of the PMAL-USPIONs in water and relevant biological media was a prerequisite for their further study *in vitro*.

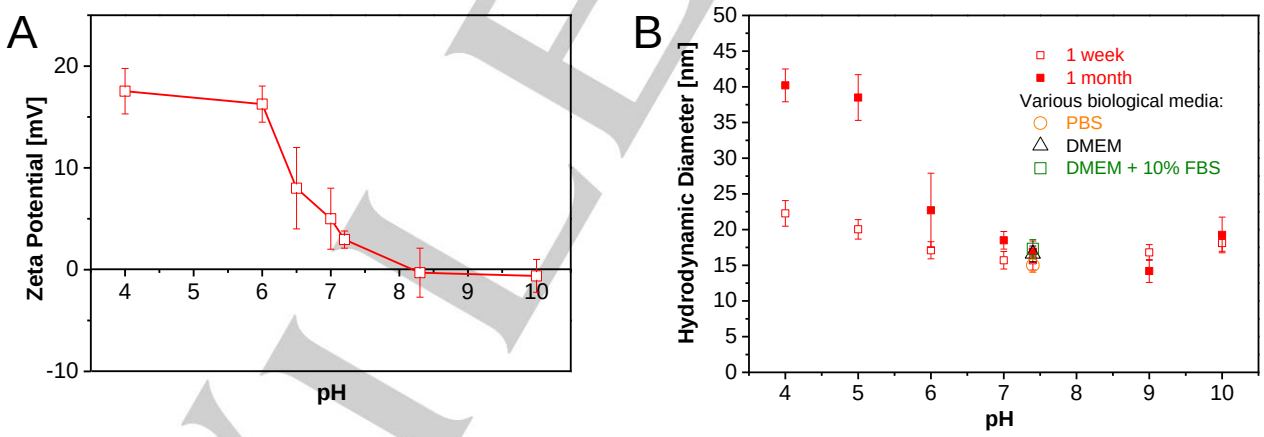

Figure 3. (A) Zeta potential of PMAL-USPIONs (in 0.05 M NaCl) measured at different pHs. (B) HD of PMAL-USPIONs at different pHs, measured after one week and one month, as well as in various biological media.

2.3 Interaction with proteins

After establishing the colloidal stability of the PMAL-USPIONs, we next focused on studying the interaction of the PMAL-USPIONs with proteins in order to gain a better understanding of the nano-bio interface, which can significantly affect the cellular uptake and pharmacokinetics of NPs.[50]

2.3.1 Impact on conformation of bovine serum albumin

In the first instance, circular dichroism (CD) spectroscopy was used to examine the interaction of the PMAL-USPIONs with a single representative protein, bovine serum albumin (BSA). CD analysis can provide valuable information on changes in the structural conformation of a protein induced by its interaction with nanoparticulate surfaces.[51] Figure S4 shows the CD spectra of BSA measured before and after incubation for 1 h with increasing concentrations of PMAL-USPIONs in 8 mM Tris-HCl (pH 7.4) buffer at 37°C. Since BSA contains predominantly α-helices as secondary structural elements, two negative bands at 208 nm and 220 nm are observed in the CD spectra. The intensity of these bands did not change upon incubation with the PMAL-USPIONs, and the isodichronic point did not shift, as has been found in cases of "hard" protein corona formation.[51] This suggests that BSA does not undergo significant structural change upon incubation with the PMAL-USPIONs.

Several groups, using different NPs, have observed NPs surface-induced denaturation of serum proteins such as fibrinogen and albumin.[52-56] Fleischer *et al.*[57] recently investigated the relationship between the NP surface charge, the secondary structure of serum proteins attached thereto and the resulting interaction of the OPA-USPIONs protein complex with cellular receptors. On one hand, a change in the secondary structure of BSA induced by cationic NPs redirects the protein-NP complex to scavenger receptors while, on the other, BSA adsorbed on anionic NPs retains its native structure, resulting in binding of BSA-NPs to albumin receptors.[57, 58] In the case of anionic NPs, a similar trend was observed for quantum dots, gold and polystyrene NPs, despite differences in diameter, material and surface modification.[59]

2.3.2 Microscopic examination of particle size in presence of proteins

Atomic force microscopy (AFM) and transmission electron microscopy (TEM) were used to evaluate the protein-nanomaterial interplay further. AFM micrographs (Figure S5) were taken of the PMAL-USPIONs and OPA-USPIONs before and after 30 min of incubation with 50% human serum (HS) at 37°C. These revealed that the negatively charged OPA-USPIONs are enveloped with serum proteins after mixing, leading to aggregation, as evidenced by the increase in size from < 20 nm to 150 nm or more (Figure S5A). The PMAL-USPIONs, however, remained as well dispersed 15–18 nm-sized particles, indicating a high resistance to protein corona formation (Figure S5B). TEM confirmed that the PMAL-USPIONs do not aggregate in the presence of serum (insert image in Figure S5B).

2.3.3 Analysis of adsorbed proteins using proteomics-based techniques

Corona formation involves both reversible and irreversible adsorption of proteins. In order to analyze the composition of the nanoparticle-protein complexes in more detail, PMAL-USPIONs and OPA-USPIONs were incubated with different concentrations of HS (5–80%). The NP-associated proteins were separated from unbound serum proteins by centrifugation, followed by extensive washing with water to remove proteins with low affinity for the nanoparticle surface. Surface-associated proteins were then detached from the NPs by heating to 95°C with 2x Laemmli sample buffer containing 2-mercaptoethanol, and analyzed by 1D sodium dodecyl sulfate-polyacrylamide gel electrophoresis (SDS-PAGE), followed by visualization of protein bands by staining with a colloidal Coomassie G-250 dye. As previously reported by Hofmann and co-workers,[60] the choice of solution used to wash the NPs after serum incubation was found to influence the results. The gels shown in Figure 4 correspond to proteins retained on the NPs after washing with water.

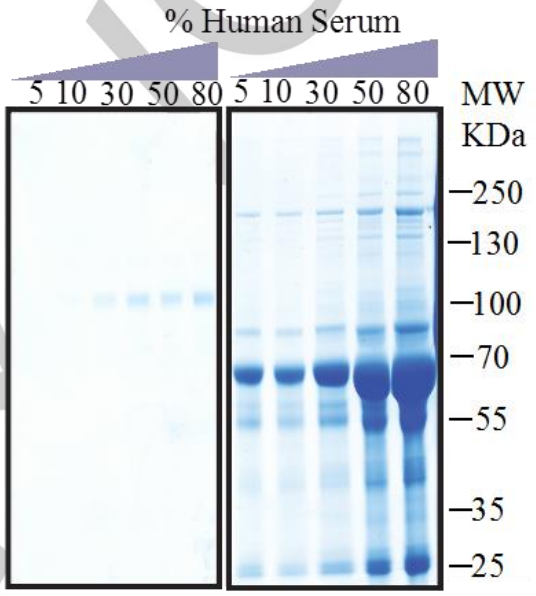

Figure 4. Colloidal Coomassie-stained 12% SDS-polyacrylamide gel of HS proteins adsorbed to PMAL-USPIONs (left) and OPA-USPIONs (right).

It is immediately obvious from Figure 4 that the PMAL-USPIONs adsorbed much less protein than the negatively charged OPA-USPIONs, again highlighting the effectiveness of a zwitterionic surface in resisting the formation of a protein corona (although this analysis does not detect the presence of a "soft" corona, *i.e.*, proteins that bind only very weakly to the surface). Hardly any protein bands could be visualized for the incubated PMAL-USPIONs, even at high serum concentrations. The most pronounced band was found at *ca.* 100 kDa. The concentration of the protein mixture to which a NP surface is exposed has previously been shown to have a strong influence on protein corona composition in some instances.[61] For the OPA-USPIONs, however, the protein corona composition did not appear to change significantly with serum concentration only that the amounts of adsorbed proteins increased. We previously found that a protein corona forms consistently around OPA-USPIONS.[41]

The identity of the NP-binding proteins was established using mass spectrometry (MS)-based techniques. The entire

SDS-PAGE lane for NPs incubated with 50% HS were divided into ten lanes followed by in-gel digestion and analyzed by liquid chromatography-tandem mass spectrometry (LC-MS/MS). For the OPA-USPIONs, a total of 28 proteins were identified with a high degree of confidence (< 1% false discovery rate (FDR) and at least 2 unique peptides per protein) and further validated through human plasma proteome database (Plasma Proteome Database) to be *bona fide* plasma proteins.[62] For the PMAL-USPIONs, only seven proteins were detected. Of these proteins, six were also identified in the corona of the OPA-USPIONs (Figures 5A). The complete list of identified proteins, including their molecular weights and isoelectric points (pI), can be found in the ESI (Tables S3 and S4).

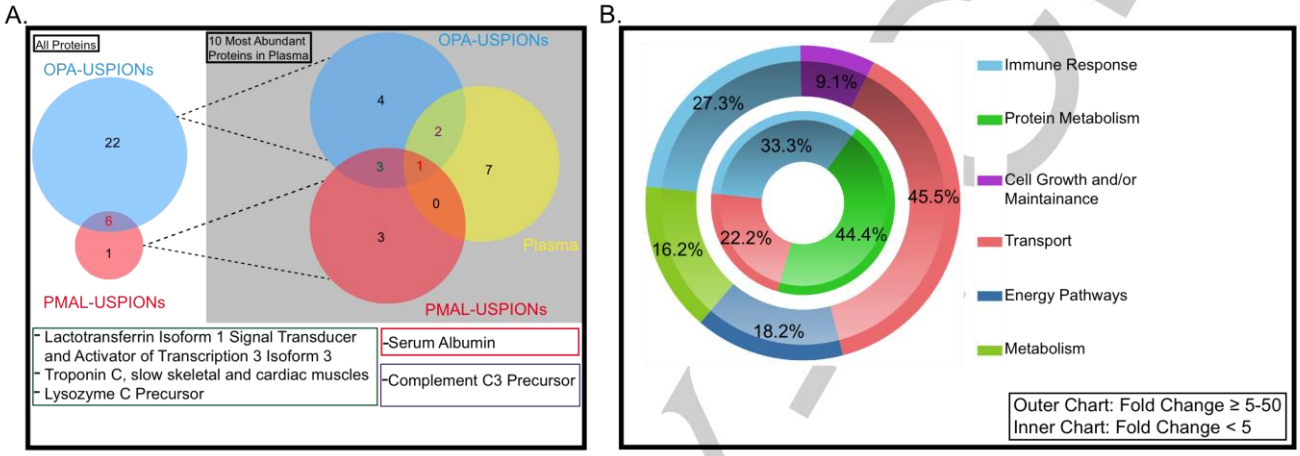

Figure 5. Bioinformatic classification of proteins identified in the coronas of 50% HS-exposed PMAL-USPIONs and OPA-USPIONs. (A) Venn diagram for all proteins identified by qualitative proteomics analysis (left) and for the ten proteins in each set with the highest Mascot protein score, together with the ten most abundant human plasma proteins (right). (B) Classification of proteins measured by quantitative proteomics analysis according to their biological function. The outer and inner charts correspond to proteins enriched 5–50-fold and < 5-fold, respectively, in the corona of serum-exposed OPA-USPIONs relative to that of PMAL-USPIONs.

Proteins of the human plasma play a crucial role in the recognition of foreign materials entering the body.[63, 64] To gain an understanding of the nature of the adsorbed proteins, we selected and ranked the ten proteins with the highest Mascot protein score (Table S5) and compared them with the ten most abundant proteins in human plasma found in the coronas of other previously studied NPs, as reported by Tenzer *et al.*[63, 64] Surprisingly, the only such serum-abundant protein that was common to both the coronas of the PMAL-USPIONs and OPA-USPIONs coronas was serum albumin. None of the other ten proteins with the highest Mascot protein score were detected in the corona of the PMAL-USPIONs (Figure 5A). For the corona of the OPA-USPIONs, however, a further two of the proteins with the highest Mascot protein score were among the ten most abundant serum proteins, namely complement C3 precursor and serotransferrin. For these OPA-USPIONs, all of the top ten proteins have a pI < 7.1, *i.e.*, they are negatively charged at physiological pH (7.4), clearly indicating that an overall negative charge does not preclude adsorption of a protein to the surface of a negatively charged particle. Similar results were reported for negatively charged silica nanoparticles.[63, 64] The overall protein corona composition for the OPA-USPIONs is strikingly similar to that reported for SPIONs coated with polyvinyl alcohol[60]. Overall,most of the proteins detected and identified in the corona of the PMAL-USPIONs were relatively low in molecular weight (< 80 kDa), while proteins up to 515 kDa in molecular weight were found in the corona of the OPA-USPIONs (Tables S3 and S4).

Relative quantification of the amounts of individual proteins found in the hard protein corona of the serum-exposed OPA-USPIONs versus that of the PMAL-USPIONs was carried out using isotope dimethyl labeling.[65, 66] Following removal of unbound and weakly bound proteins by washing, the adsorbed proteins were detached using a denaturant containing 8 M urea, reduced and labeled with non-deuterated (“light”) and deuterated (“heavy”) formaldehyde separately. The labeled proteins were then mixed in equal amounts and analyzed by LC-MS/MS.[65] A total of 21 proteins were quantified for the NPs incubated in 50% HS, as shown in Table S6. The majority of proteins (17) were present in greater amounts in the corona of the OPA-USPIONs versus that of the PMAL-USPIONs.

A functional enrichment tool, FunRich, was next used to classify the bound proteins according to their biological function.[67] Of the proteins that were enriched by a factor of 5–50 in the corona of the 50% HS-exposed OPA-USPIONs versus that of the PMAL-USPIONs, about 30% are associated with the immune response, 45% with transport, and the rest with metabolism and energy (Figure 5B). The proteins that were enriched by factors ≤ 5, are mostly associated with the immune system, protein metabolism and transport. Thus, the biological function analysis revealed a significant enrichment of plasma proteins involved in complement activation and coagulation, as

well as lipoproteins, for the OPA-USPIONs, consistent with findings for other negatively charged nanoparticles.[63, 64]

2.4 Biocompatibility studies

The toxicity of engineered NPs (nanotoxicity) can be assessed by a multitude of different functional assays and viability assays.[68, 69] Regarding the latter, we investigated the metabolic activity of cancerous and non-cancerous cells to determine their viability following nanoparticle exposure, and assessed their membrane integrity by monitoring the OPA-USPIONs induced leakage of active lactate dehydrogenase (LDH) into the cell culture media. Since PMAL-USPIONs are intended to be directly injected into the bloodstream, we also analyzed the lysis of human erythrocytes in response to NPs and tested their ability to induce cytokine secretion from peripheral blood mononuclear cells.

2.4.1 Hemolytic activity

As there is a risk that NP coatings can disrupt the membranes of red blood cells (RBCs),[70] we studied the hemolytic activity of PMAL-USPIONs in the presence and absence of serum over 60 min, comparing it with the activity of OPA-USPIONs. Both NP species were incubated with RBCs isolated from heparin-stabilized human blood. The results (Figures 6 and S6) demonstrate the biocompatibility of PMAL-USPIONs towards RBCs as there was no significant release of hemoglobin detectable upon incubation of RBCs with these NPs. No considerable time- or concentration-dependent hemolytic response was observed, either in the presence or absence of serum. These results clearly indicate that the cell membranes of RBCs were not disrupted by PMAL-USPIONs at concentrations ≤ 150 nM, representing the critical concentration used for *in vivo* studies. In contrast, a dose- and time-dependent increase in hemolysis was observed for the OPA-USPIONs. Interestingly, the hemolytic activity of the OPA-USPIONs was significantly mitigated in the presence of serum, corroborating recent reports that the formation of a protein corona reduces the hemolytic potential of NPs.[23, 71] Notably, the supernatants obtained after centrifuging the USPIONs-RBC mixtures were brown in color, with no evidence of NP precipitation (Figure S7). This indicates that the NPs remained suspended in solution and that the amphiphilic polymer coatings were stable in blood over the course of the experiment, since their dissociation would have led to NP aggregation and precipitation.

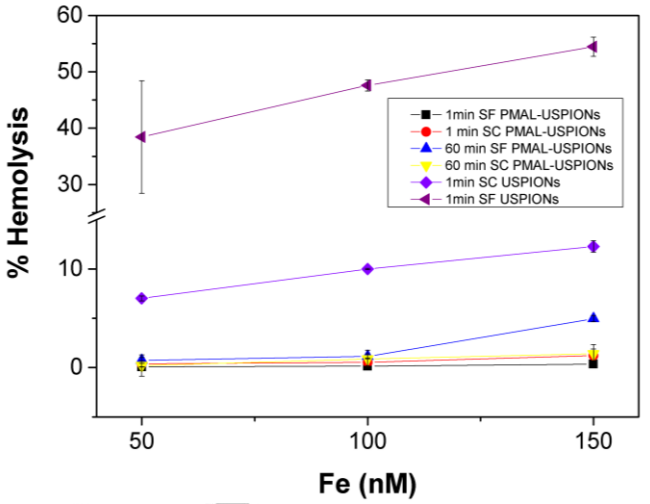

Figure 6. Hemolytic activity of PMAL-USPIONs and USPIONs measured at different concentrations (as represented by the iron concentration) and time points in the presence and absence of serum (n = 3). SF = serum-free, SC = serum-containing.

2.4.2 Cytokine response

In order to predict the systemic cytokine response to the PMAL-USPIONs, a human whole blood cytokine release assay was utilized in combination with a sandwich-based enzyme-linked immunosorbant assay (ELISA) to simultaneously detect several inflammatory and immunoregulatory cytokines and chemokines. Whole blood anticoagulated with heparin was incubated with PMAL-USPIONs at two different concentrations and the release of interleukines IL-1α, IL-1β, IL-2, IL-4, IL-6, IL-8, IL-10, IL-12 and IL-17A, as well as interferons (IFN-γ), tumor necrosis factors (TNF-α) and granulocyte/monocyte colony stimulating factors (GM-CSF), was monitored. As shown in Figure S8, incubation of blood cells with PMAL-USPIONs for 4 h did not induce a change in cytokine or chemokine levels compared to untreated control cells. Since all inflammatory mediators remained in the clinical reference range, it can be concluded that PMAL-USPIONs are unlikely to cause an inflammatory response or adverse side effects *in vivo*, and that these nanoscale materials can be regarded as non-immunotoxic.[72]

2.4.3 *In vitro* toxicity

To assess cell viability following PMAL-USPIONs exposure, the metabolic activities of cancerous and non-cancerous cells represented by human squamous carcinoma (A431) and human embryonic kidney (HEK 293) cells, respectively, were assayed for a period of 24 h. In addition to the percentage of metabolically active cells, their membrane integrity as a measure of viability and necrosis was assessed by monitoring the PMAL-USPIONs-induced leakage of active LDH into the cell culture

media. The results (Figure 7) reveal that the cellular metabolism of both cell lines is not substantially affected by exposure to a concentration of 100 µg/mL PMAL-USPIONs.

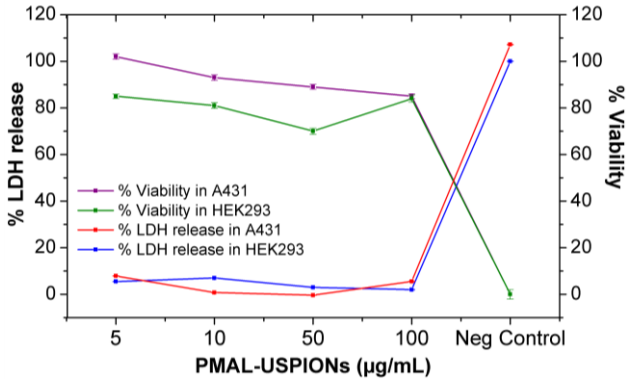

Figure 7. Cellular metabolism and lactate dehydrogenase (LDH) release as a measure of viability and necrosis, respectively, of cancerous (A431) and non-cancerous (HEK293) cells after exposure to PMAL-USPIONs for 24 h. For the LDH assay, a triplicate set of wells was incubated with supplied lysis buffer to obtain maximum LDH release (positive control). PMAL-USPIONs-dependent LDH release was calculated relative to this value. In the viability assay, a triplicate set of wells containing untreated cells served as negative control. Cell viability upon PMAL-USPIONs exposure was expressed as a percentage relative to this negative control.

Furthermore, for both cell lines, release of LDH was in the same range of the negative control for all NP concentrations tested. From the two tests, we conclude that PMAL-USPIONs do not have any obvious toxicity towards the investigated cell lines under the examined conditions.

2.5 Cellular interaction

2.5.1 Uptake by macrophages and liver cells

In order to investigate the potential for phagocytic uptake of PMAL-USPIONs by macrophages, the human monocytic leukemia cell line THP-1 was used. THP-1 cells can differentiate into monocyte-derived macrophages. In parallel, the HepG2 (liver hepatocellular carcinoma) cell line was investigated in order to assess the potential for liver uptake of the NPs *in vivo*. To follow the intracellular pathway of the PMAL-USPIONs, a fluorescent dye (Cy5) bearing an amine pendant group was attached to the surface of the NPs *via* standard EDC/NHS-mediated amide bond formation, with a loading of approximately four Cy5 molecules per NP (see Experimental Section for details). The Cy5-PMAL-USPIONs were incubated with both cell lines at a concentration of 20 µg/mL for different period of time. The cells were fixed and subsequently imaged by confocal fluorescence microscopy. As shown in Figure 8, the time-dependent uptake of the Cy5-PMAL-USPIONs by THP-1 cells (Figure 8A) was found to be very weak compared to the uptake of Cy5-OPA-USPIONs (Figure 8B), indicating that the largely corona-free zwitterionic coating provides a high degree of protection against macrophagocytosis.[73] A blocking experiment with maleylated BSA (mal-BSA), a well-known polyanionic ligand for scavenger receptors (SRs), was performed in order to see if the low uptake of the Cy5-PMAL-USPIONs was SR-mediated. This revealed that some NPs may indeed be internalized *via* this route, as evidenced by the reduction in observed fluorescence.

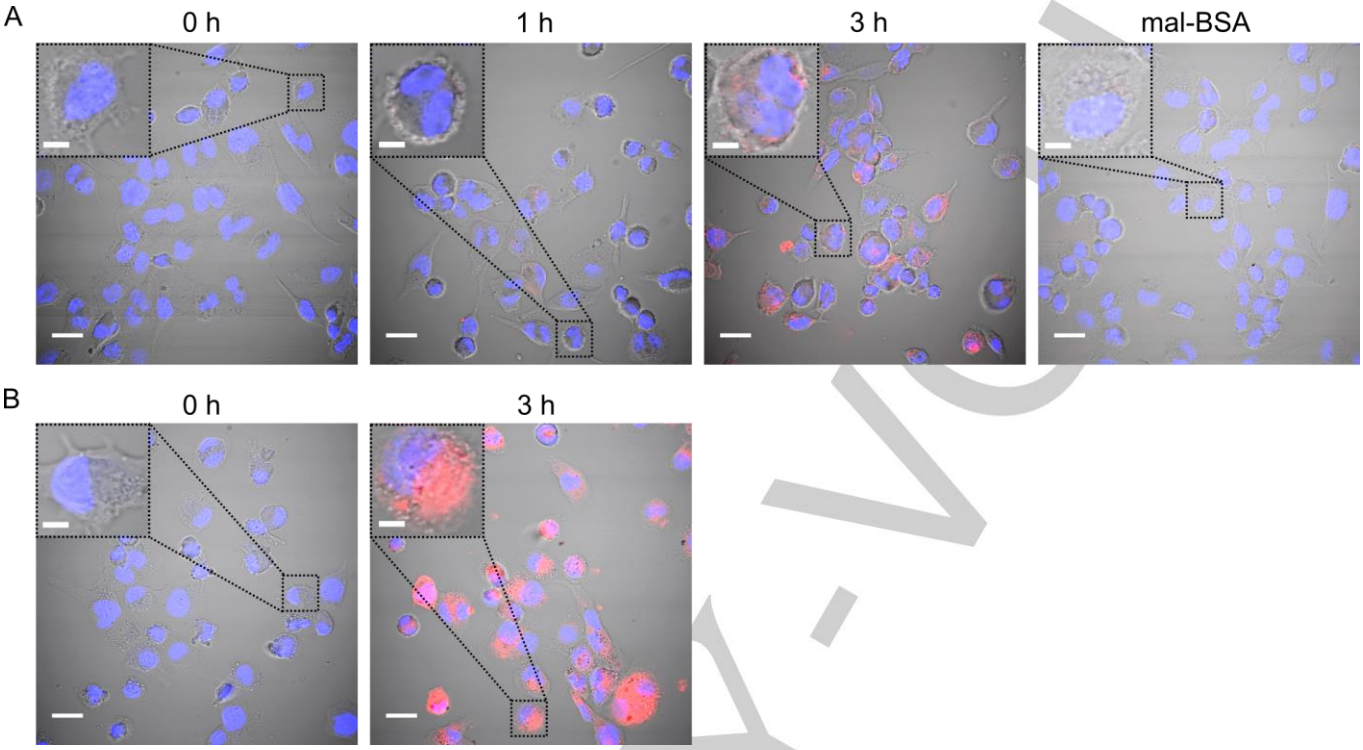

Figure 8. Confocal fluorescence images of NP uptake by THP-1 cell derived macrophages. (A) THP-1 macrophages incubated with Cy5-PMAL-USPIONs for 0 h (control), 1 h, 3 h, or 1 h after blocking of scavenger receptors with 36 µM maleylated BSA (mal-BSA). (B) THP-1 macrophages incubated with Cy5-OPA-USPIONs for 0 h (control) and 3 h. The concentration of the NPs was 20 µg/mL. The red fluorescence is from the Cy5 dye attached to the NPs. Cell nuclei were stained with Hoechst 33258 (blue). Scale bar = 20 µm. Inset scale bar = 5 µm.

Uptake of the Cy5-PMAL-USPIONs into HepG2 cells was also found to be very low (Figure 9), contrasting with the significant uptake reported for zwitterionic dopamine-coated magnetite NPs at similar concentrations to those employed here.[28] This suggests that zwitterionic-polymers may be more effective in securing NPs from recognition and scavenging by the MPS.[28]

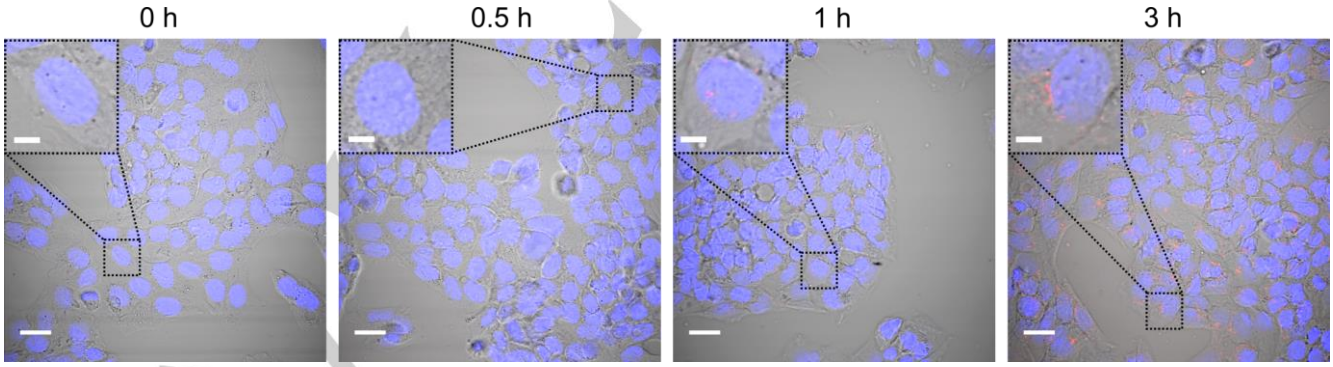

Figure 9. Confocal fluorescence images of HepG2 cells incubated with Cy5-PMAL-USPIONs for 0 h (control), for 0.5 h, 1 h and 3 h. The concentration of the NPs was 20 µg/mL. The red fluorescence is from the Cy5 dye attached to the NPs. Cells nuclei were stained with Hoechst 33258 (blue). Scale bar 20 µm. Inset scale bar = 5 µm.

2.5.2 Uptake by non-phagocytic cells

Uptake of the PMAL-USPIONs by non-phagocytic cells was also investigated. This involved incubation of the NPs with cancerous (A431) and non-cancerous (HEK293) cells for 24 h, either in the absence or presence of different concentrations of fetal bovine serum (FBS) or HS, followed by ICP-MS analysis to quantify the concentration of Fe arising from the magnetite core of the NPs (prior experiments performed in the absence of NPs confirmed that the cells were able to grow under all conditions examined). Studies were performed under both serum-containing and serum-free media conditions in view of the fact that cellular uptake of NPs has been shown to be significantly affected by the presence of a protein corona.[74, 75] For comparative purposes, the uptake of OPA-USPIONs was also examined. As shown in Figure 10, the degree of uptake of the USPIONs is dependent on the cell type, the NPs surface coating and the concentration of serum. Notably, no uptake of PMAL-USPIONs was observed for either cell line in serum-free or serum-containing media, once again highlighting the effectiveness of the zwitterionic PMAL coating in conferring "stealth" properties to the NPs. In contrast, internalization of the negatively charged OPA-USPIONs was significant in the absence of serum, as previously reported by us.[41] The level of uptake was reduced in the presence of serum, which is concordant with findings for other NPs with a negative surface charge.[58] The lack of free proteins and a protein corona under serum-free conditions may be facilitating the cellular uptake of the OPA-USPIONs, whereas a competitive process hinders uptake when serum proteins are present.

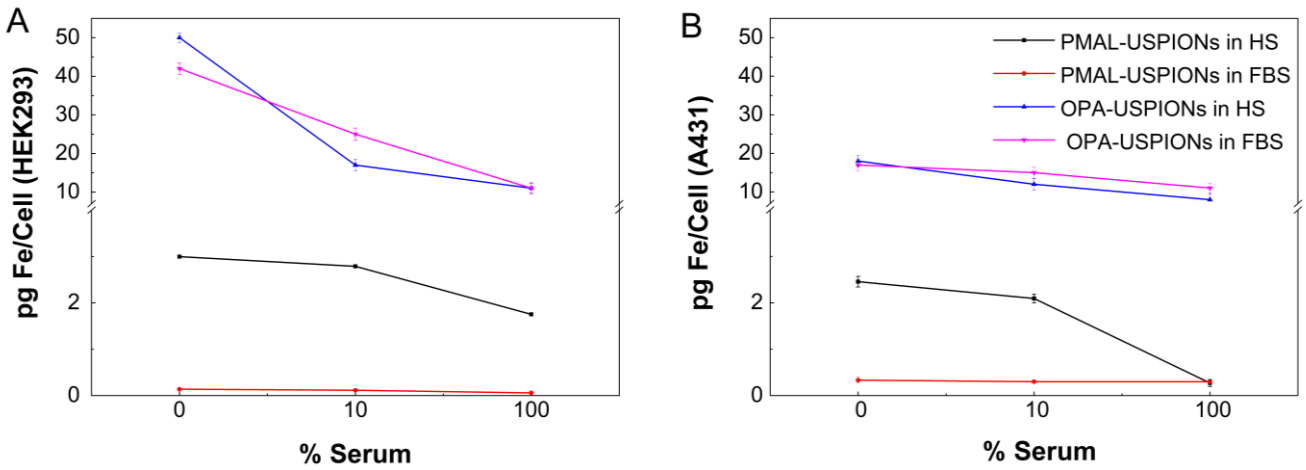

Figure 10. Degree of uptake of PMAL-USPIONs and OPA-USPIONs into (A) A431 and (B) HEK293 and cells after 24 h incubation, either in the absence or presence of 10 or 100% of FBS or HS.

Conclusions

We have demonstrated that coating of oleic acid/oleyl alcohol-stabilized USPIONs with zwitterionic PMAL polymer confers excellent colloidal stability and anti-fouling properties on the resulting water-dispersible NPs, even in undiluted serum. PMAL-USPIONs exhibit minimal cytotoxicity and only very low levels of cellular uptake across a range of cell lines, including macrophages and hepatocarcinoma cells. Moreover, they do not elicit an inflammatory cytokine response or exhibit hemolytic activity *in vitro*. Overall, PMAL-USPIONs represent a potentially promising platform for the development of new bio-imaging/therapeutic agents with fewer off-target effects.

Experimental Section

Materials

All chemicals were purchased from commercial suppliers and used as received without further purification. Oleic acid (99%), oleyl alcohol (99%), diphenyl ether (≥ 99%), poly(maleic anhydride-alt-1-decene) modified with 3-(dimethylamino)propylamine (PMAL-C8, M_w = 18.5 kDa), *N*-(3-dimethylaminopropyl)-N'-ethylcarbodiimide hydrochloride (EDC), *N*-hydroxysulfosuccinimide sodium salt (sulfo-NHS), *tris*(2-carboxyethyl)phosphine hydrochloride (TCEP) 2-(*N*-morpholino)ethanesulfonic acid (MES), sodium monohydrogen phosphate anhydrous (Na_2HPO_4), sodium dihydrogen phosphate dihydrate ($NaHPO_4$ 2 H_2O), nitric acid (HNO_3, 69% ultrapure) and trifluoroacetic acid (TFA, 99%) were purchased by Sigma Aldrich. Cyanine-5-amine was purchased from Lumiprobe. Dimethyl sulfoxide

(DMSO, 99%), methanol (99%), ammonium acetate (NH_4OAc, 99%) and acetonitrile (CH_3CN) were purchased by Merck. Ultrapure water 18 Ω cm was obtained from an inline Millipore RiOs/Origin System (Millipore Corporation, USA). Iron(II) oleate complex was prepared according the published procedure.[76] OPA-USPIONs were synthesized as previously described.[41]

Synthesis of oleic acid/oleyl alcohol-stabilized USPIONs

The protocol reported by Hyeon *et al*.[42] was modified slightly to produce 5 nm-sized USPIONs. Briefly, the iron(II) oleate complex (370 mg, 0.6 mmol), oleic acid (170 mg, 0.6 mmol) and oleyl alcohol (500 mg, 1.82 mmol) were dissolved in diphenyl ether (4.0 g, 3.7 mL). The mixture was heated to 250°C at a rate of 7.5°C/min to initiate NP formation, and then kept at this temperature for 30 min under an inert N_2 atmosphere. After cooling to room temperature (RT), acetone (20 mL) was added, the precipitated NPs pelleted by centrifugation (4,000 rpm, 30 min), and the supernatant discarded. This procedure was repeated four times. The final pelleted USPIONs were dissolved and stored in chloroform.

PMAL coating of USPIONs and purification

PMAL (45 mg) was mixed with the oleic acid/oleyl alcohol-stabilized USPIONs (5 mg) in chloroform (5 mL) for 1 h at RT. The solvent was then slowly removed with a rotary evaporator and the residue further dried with a N_2 stream, leading to the formation of a thin film of PMAL-USPIONs plus excess PMAL. The film was dissolved in 50 mM borate buffer (pH 8.5) or water (4 mL) and sonicated for 15 min. Free PMAL polymers were removed by washing with water three times. Between each wash, the NPs were pelleted by ultracentrifugation (174,000 × g for 4 h) using a fixed angle rotor (90Ti, Optima XPN-80 ultracentrifuge, Beckman Coulter). The PMAL-USPIONs were then resuspended in water or borate buffer (purified by filtration through 0.2 µm syringe filters (Pall)) by slight agitation in an ultrasonic bath. Minor amounts of 50–500 nm-sized aggregates were removed by two subsequent ultrafiltration steps (Viva Spin 6, polyethersulfone (PES) membranes, Sartorius, MWCO 1,000 and 300 kDa, corresponding to pore sizes of 18 and 12 nm for globular particles[77, 78]) using ultrapure water (Figure S2). The ultrafiltrates were concentrated by 30 kDa filtration devices with < 5 nm pore size (Vivaspin 6, Satorius). The achieved final concentrations of 1–5 g/L Fe, corresponding to 2.5–12.5 g/L PMAL-USPIONs were measured by inductively-coupled plasma mass spectrometry (ICP-MS, ELAN 9000, Perkin Elmer). The measurements were done with internal Rhodium-standard and calibration was performed before measurement with ICP standard solutions, *e.g.*, Fe in 0.5 M HNO_3 (Bernd Kraft GmbH).

Particle characterization techniques

Bright-field TEM and high-resolution TEM (HRTEM) micrographs were collected on a Titan 80-300 (FEI) microscope operating at an accelerating voltage of 300 kV. Samples of the PMAL-USPIONs were dried on carbon-coated copper grids under ambient conditions. XRD analysis of dried PMAL-USPIONs was performed on a Bruker D8 diffractometer using Cu Kα radiation. The size of the crystallites was determined from the line broadening at half of the maximum intensity (FWHM) of the (311) reflection by application of the Debye-Scherrer equation.[44] The hydrodynamic diameter (HD) of the NPs was determined by dynamic light scattering (DLS) and zeta potential was determined by Laser Doppler velocimetry (Zetasizer Nano ZS Malvern Instruments, UK). Thermogravimetric analysis (TGA) was applied to determine the mass percentage of oleic acid/oleyl alcohol and PMAL in the purified PMAL-USPIONs (air atmosphere, heating rate 5 K/min, 25–600°C, Sensys TG-DSC, Setaram, France). Pure PMAL and oleic acid/oleyl alcohol-stabilized USPIONs were used as references. Elemental analysis was performed on a EuroEA 3000 instrument from EuroVector (Milan, Italy). The quantity of carboxylic acid groups on the PMAL-USPIONs surface was estimated by potentiometric titration (736 GPTitrino, Metrohm). The solid samples (5–10 mg) were suspended in degassed water (50 mL) and titrated by addition of 0.01 M NaOH/HCl (VWR) at pH 3–10 under an inert atmosphere.

Conjugation of Cy5 fluorescent dye to PMAL-USPIONs and OPA-USPIONs

PMAL-USPIONs (1 mg) containing 0.9 µmol of COOH were activated for 15 min with a 20-fold excess of EDC (18 µmol) in 250 µL MES buffer (pH 6, 0.1 M). Sulfo-NHS (18 µmol) dissolved in 0.1 M phosphate buffer (250 µL, pH 7) was then added and the mixture shaken for 15 min. Cyanine-5-amine (0.09 µmol) dissolved in DMSO (20 µL) was then added dropwise to the activated NPs (corresponding to a 1:10 Cy5-to-COOH molar ratio), and the volume adjusted up to 1 mL with the 0.1 M phosphate buffer (pH 7). The reaction mixture was shaken overnight at room temperature. The reaction progress was monitored by TLC analysis using silica gel $60F_{254}$ (Merck) and a 1:1 (v/v) MeOH/2 M NH_4OAc eluent system (free Cy5: R_f = 0.6, Cy5-PMAL-USPIONs: R_f = 0). The Cy5-PMAL-USPIONs were purified using a Sephadex G-25 column (PD-10), with 0.1 M phosphate buffer (pH 7) used to remove the unreacted coupling agents and cyanine-5-amine. The collected Cy5-PMAL-USPIONs fractions were concentrated *via* spin filtration (4,000 g for 20 min) with Amicon filter (MWCO 30,000). The presence of the conjugated Cy5 was clearly evident from the blue color of the NPs and characteristic UV-Visible (λ_{max} = 646 nm) and fluorescence (λ_{max} = 665 nm) spectra. The fluorescence λ_{max} is slightly red-shifted with respect to the free fluorophore, as already reported for other dye-nanoparticle interfaces.[79] Based on the measured absorption spectrum of the Cy5-PMAL-USPIONs, approximately four Cy5 molecules were attached to each NP. Cy5-labeled OPA-USPIONs were prepared in an analogous fashion.

Circular dichroism spectroscopy (CD)

CD spectra were recorded with a J-815 spectrometer (JASCO, Gross-Umstadt, Germany) equipped with a continuously stirred, temperature-controlled 1 cm-path length cuvette. An average of ten scans was recorded within a wavelength range of 190–290 nm, using a bandwidth of 1 nm. The bovine serum albumin (BSA, AppliChem) concentration was constant at 3 µM and the concentration of PMAL-USPIONs was varied from 10 to 100 µg/mL. BSA and NPs were incubated for 30 min at 37°C before measurement.

Atomic force microscopy (AFM)

AFM was performed using a Multimode 8scanning probe microscope (Bruker) and PP-NCLR cantilevers from Nanosensors (nominal force constant 48 N m^{-1}, tip radius < 10 nm). Images were processed using Gwyddion open source software. Samples were prepared by adding 20 µL of a 30 µg/mL stock of NPs, previously incubated for 30 min at 37°C with water or human serum (HS) to a freshly-cleaved mica surface and air-drying before imaging.

Protein isolation from NP surfaces and sodium dodecyl sulfate polyacrylamide gel electrophoresis (SDS-PAGE)

PMAL-USPIONs and OPA-USPIONs were incubated in HS at different dilutions for 30 min at 37°C. After incubation, serum-NP mixtures were centrifuged for 4 h at 20,000 x g. In each case, the supernatant was

carefully removed and the pellet washed four times with PBS (1 mL) by suspension in solution followed by pelleting and removal of supernatant (a serum-only sample showed no sedimentation of free proteins under such conditions). Proteins were eluted from the NP surfaces by adding 2x Laemmli Sample Buffer (Bio-Rad) with 2-mercaptoethanol to the final pellets and subsequent incubation at 95°C for 5 min. For SDS-PAGE, recovered proteins in sample buffer (20 µL) were separated on a 4–12% SDS-PAGE gel (NuPAGE®, Invitrogen). PageRuler™ Plus Prestained Protein Ladder (Thermo Scientific) was used as marker and 1x MOPS (Invitrogen) as running buffer. Gels were run at 120 V for 1.3 h and Coomassie staining (InstantBlue™, Expedeon) was performed to visualize the bands.

In-gel tryptic digestion

The entire SDS-PAGE gel lane was sliced into *ca.* 1 mm^3-sized cubes using a clean scalpel, and destained overnight in a 1:1 (v/v) mixture of CH_3CN and 50 mM triethylammonium bicarbonate (TEAB) buffer. The gel pieces were then washed twice with 100% CH_3CN for 30 min. The proteins present were reduced with 2.5 mM TCEP at 55°C for 45 min, followed by alkylation with 10 mM iodoacetamide in the dark at RT for 30 min. The gel pieces were then washed twice with 50 mM TEAB, followed by 100% CH_3CN. Digestion was carried out by incubating the gel pieces in a 20 mM TEAB solution containing 0.5 µg of trypsin (Promega Corp.) at 37°C overnight. Formic acid was then added to a final concentration of 1% (v/v) before mass spectrometric analysis.

Mass spectrometry and data analysis

Tryptic digests were analyzed by LC-MSMS using a LTQ Orbitrap Elite (Thermo Scientific) with a nanoelectrospray interface coupled to an Ultimate 300 RSLC nanosystem (Dionex) The nanoLC system was equipped with an Acclaim Prepmap Nanotrap column (Dionex C18, 100 Å, 75 µm x 2 cm) and an Acclaim Pepmap analytical column (Dionex C18, 2 µm, 100 Å, 75 µm x 15 cm). An aliquot of the digestion mix (2 µL) was loaded onto the trap column with an isocratic flow of 4 µL min^{-1} of 3% CH_3CN containing 0.1% formic acid for 5 min before the enrichment column was switched in-line with the analytical column. The eluents used for the liquid chromatography were 0.1% (v/v) formic acid (solvent A) and 100% CH_3CN/0.1% formic acid (v/v) (solvent B). The following gradient was used: 3% to 12% for 1 min, 12% to 35% B for 20 min, 35% to 80% B for 2 min, and then constant 80% B for 2 min, followed by equilibration at 3% B for 7 min before the next sample injection. The LTQ Orbitrap Elite mass spectrometer was operated in the data-dependent mode with a nano ESI spray voltage of +2.0 kV, a capillary temperature of 250°C, and an S-lens RF value of 60%. Spectra were acquired first in positive mode with full scan, scanning from *m/z* 300 to 1650 in the FT mode at 240000 resolution followed by collision-induced dissociation in the linear ion trap with the ten most intense peptide ions with charge states ≥ 2 isolated and fragmented using a normalized collision energy of 35 and an activation Q of 0.25. Data were analyzed using Proteome Discoverer (Thermo Scientific version 1.4) with Mascot (Matrix Science version 2.4) against the human RefSeq database. Search results were set to a maximum of 1% false discovery rate, with two unique peptides required for positive identification.[73] To selectively filter plasma proteins, Plasma Proteome Database was used.

Relative quantitative dimethyl labeling

For the relative quantitative protein analysis, PMAL-USPIONs and OPA-USPIONs were incubated in triplicate with 50% HS for 30 min at 37°C. Protein isolation was performed in the same way as described for the SDS-PAGE. Detachment of the bound proteins from the corona of the NPs was achieved using 8 M urea in 25 mM TEAB. The proteins were then reduced, alkylated and digested using sequencing grade trypsin, and labeled with formaldehyde (CH_2O for PMAL-USPIONs and CD_2O for OPA-USPIONs) following a previous protocol published by Boersema *et al*.[65] Finally, both labeled samples were mixed and analyzed by LC-MS/MS as described above. Relative quantitation between both samples was carried out by extracting and comparing the area of the light and heavy labelled peptides. Data analysis was performed using Proteome Discoverer (Thermo Scientific, version 1.4) with Mascot search engine (Matrix Science version 2.4) against the Uniprot database for the human genome. The search parameters included a precursor mass tolerance of 20 ppm, fragment mass tolerance of 0.2 Da, carbamidomethyl of cysteine as fixed modification, and dimethyl labeling (CH_2O + 28.031 Da; CD_2O + 32.056 Da) at the peptide N-terminus and lysine set as variable modifications. Trypsin with no missed cleavages was used as the cleavage enzyme. Search results were set to a maximum of 1% false discovery rate (FDR) and at least two unique peptides. Quantification of the dimethyl-labeled peptides was conducted using the Quant node on Proteome Discoverer. To add further confidence proteins were filter against the human plasma proteome database.[62] Bioinformatic analysis to identify biological functions was performed using FunRich as previously described.[67]

Sampling of human blood and preparation of plasma

Blood was drawn by a trained phlebotomist under the supervision of a qualified and licensed physician following the guidelines of the HUPO Plasma Proteome Project (HUPO PPP) through venipuncture from healthy female and male volunteers and collected into heparin containing tubes (S-Monovette®, Sarstedt).[80] Immediately after blood sampling, each tube was inverted ten times to ensure thorough mixing of blood with heparin. After centrifugation of the tubes for 10 min at 1,000 x g at 4°C, equal volumes of plasma from each donor were collected into a secondary 50 mL conical bottom Falcon tube and subsequently centrifuged at 2,400 x g for 15 min at 4°C. The supernatant was transferred into a new 15 mL Falcon tube and stored at 4°C until use.

Hemolytic activity assessment

Red blood cells (RBCs) were isolated from heparin-stabilized human whole blood by three cycles of centrifugation and dilution in PBS (300 x g, 10 min). The purified RBCs were then diluted in PBS (1 mL) and kept on ice during sample preparation. For comparative purposes, parallel experiments were performed in the presence as well as absence of blood plasma. Therefore, USPIONs were either diluted in PBS or in blood plasma, respectively, and pre-incubated for 30 min at 37°C before their addition to the RBCs. After pre-incubation, RBCs (0.5 mL) were added to the NP dispersion (10 µL) and mixed. RBCs were also incubated with PBS or water as negative or positive control, respectively. All USPION samples, as well as controls, were prepared in triplicate. The different samples were incubated for 1 min or 60 min at 37°C with shaking. After incubation, the samples were centrifuged (300 x g, 20 min) and 100 µL of supernatant transferred to a 96-well plate. The absorbance was measured at 570 nm using 655 nm as reference baseline.

The degree of hemolysis was calculated *via* the following formula:

% hemolysis = 100 * (sample – negative)/(positive – negative)

where “negative” and “positive” represent the absorbance of controls with PBS or water, respectively, and “sample” stands for the absorbance of an RBC sample incubated with USPIONs.

***In vitro* assessment of direct immunotoxicity**

Heparin-stabilized whole blood (1 mL) was incubated with different concentrations of USPIONs (50 µg/mL or 100 µg/mL) for 4 h at 37°C with gentle agitation. After incubation, the samples were centrifuged for 10 min at 1,000 x g and 4°C. The resulting plasma-containing supernatant (650 µL) represented the starting material for the Human Inflammatory Cytokines Multi-Analyte ELISArray™ Kit (Qiagen), which was used to monitor a potential USPION-induced change in cytokine levels. Following the manufacturer's instructions, relative amounts of IL-1α, IL-1β, IL-2, IL-4, IL-6, IL-8, IL-10, IL-12, IL-17A, IFN-γ, TNF-α, and GM-CSF compared to the PBS- treated blood sample (negative control) were determined and expressed as fold induction.

Cell culture

Cell culture flasks, dishes and plates (CELLSTAR®) were supplied by Greiner Bio-One GmbH. The epidermoid human cancer cell line A431 (ATCC® number: CRL-1555) and the human embryonic kidney cell line HEK293 (DMSZ number: ACC 305) were cultured as previously reported.[81, 82] The human monocytic THP-1 cells of a leukemia patient (ECACC) and the human liver hepatocellular carcinoma HepG2 cells (ATCC® number: HB-8065™) were both cultured in RPMI 1640 medium supplemented with 10% fetal calf serum and 1 U/mL penicillin/streptomycin. All cell lines were confirmed to be mycoplasma-negative using the LookOut mycoplasma PCR detection kit (Sigma-Aldrich) and were tested monthly.

***In vitro* assessment of nanotoxicity**

To assess cell viability following nanoparticle exposure, the A431 and HEK293 cells were seeded in 96-well plates at a density of 40,000 cells/0.1 mL/well and 60,000 cells/0.1 mL/well, respectively, and grown for 24 h prior to addition of PMAL-USPIONs, which were freshly diluted to different final concentrations (0, 5, 10, 50, 100 µg/mL) in DMEM supplemented with 10% FBS. After 24 h incubation, the CellTiter 96® AQueous One Solution Cell Proliferation Assay (Promega) as well as the CytoScan™ LDH Cytotoxicity Assay (G -Biosciences) were performed according to the manufacturer's instructions. For the latter assay, a triplicate set of wells were incubated with supplied lysis buffer to obtain maximum LDH release (positive control). PMAL-USPIONs-dependent LDH release was calculated relative to this value. In the proliferation assay, a triplicate set of wells containing untreated cells served as negative control. Cell viability upon PMAL-USPIONs exposure was expressed as a percentage relative to this negative control. All experiments were preformed three times.

Uptake by THP-1 derived macrophages and HepG2 cells

THP-1 cells were differentiated into macrophage like cells with 64 nM 12-O-tetra-decanoylphorbol-13-acetate (TPA) for 72 h. The differentiated THP-1 macrophages, cultured on chamber slides (Corning®), were washed once with PBS and incubated with 20 µg/mL of Cy5-PMAL-USPIONs, Cy5-OPA-USPIONs or with serum-free culture medium only for 0.5, 1 and 3 h. HepG2 cells (2 x 10^5) were seeded into each well of a chamber slide, cultured overnight, then treated with 20 µg/mL Cy5-PMAL-USPIONs in the same way as the THP-1 macrophages. To investigate the influence of a scavenger receptor (SR)-mediated uptake by THP-1 macrophages, SRs were blocked with maleylated bovine serum albumin (mal-BSA). To prepare mal-BSA, 225 mg bovine serum albumin (Sigma-Aldrich) was solved in 25 mL Tris-HCl solution (pH 8.4). About 1 g maleic anhydride (Merck) was added slowly while the pH was continuously adjusted to 8.4 using Na_2CO_3 (Roth). The solution was dialyzed (Roth, MWCO 14,000) twice for 24 h with PBS at 4°C in the dark. The protein concentration was determined with the Pierce BCA Protein Assay (Thermo Scientific), based on the Bradford protein assay. For SR blocking, the cells were pre-incubated with 36 µM mal-BSA in serum-free medium for 30 min at 37°C, before NPs were added for 1 h. After washing twice with serum-free medium and once with PBS, the cells were fixed with 4 wt.-% paraformaldehyde and 2.5 wt.-% sucrose in PBS for 40 min at RT. Then the cells were washed three times with PBS and cell nuclei were counterstained with 10 µg/mL Hoechst 33258 (Sigma-Aldrich). The samples were mounted with Fluorescence Mounting Medium (Dako) and sealed with nail polish. The imaging was performed with the Fluoview 1000 confocal laser scanning microscope (Olympus) using a 60x (NA 1.35) oil objective. The Cy5 fluorescence was acquired with a laser power of 15% and a PMT voltage of 846 V. The excitation wavelength for Hoechst 33258 was 405 nm and for Cy5 635 nm. Images were taken in sequential mode using Kalman averaging of four scans.

Quantification of uptake by HEK293 and A431 cells

A total of 200,000 A431 cells or 600,000 HEK293 cells were seeded in 12-well plates (CELLSTAR®, Greiner Bio-One GmbH) and cultivated for 24 h before exposure to nanoparticles. After 24 h, media was replaced with USPION dispersions (final concentration of 100 µg/mL), freshly prepared by diluting a USPIONs stock in serum-free DMEM, or DMEM supplemented with different concentrations of fetal calf or human serum. Following exposure to USPIONs for a time period of 24 h, cells were washed three times with PBS in order to ensure removal of loosely attached USPIONS from the cell membrane. To determine cell numbers, cells were harvested by trypsinization and counted using a CASY cell counter (Roche Diagnostics) according to the manufacture's protocol. To measure the cellular iron content by ICP-MS, cells were lysed by adding 500 µL of 0.1% NaOH, dissolved by adding 100 µl of 65% HNO_3 and finally diluted to 2 mL with dH_2O prior to analysis. The iron content was is expressed in pg Fe/cell. Cells without USPION treatment served as controls for calculations.

Acknowledgements

We thank Dr Jörg Grenzer for the XRD measurements, Dr Elisabeth Fischmeier and Bezu Teschome for instrumental help with CD and AFM respectively. We thank Utta Herzog for excellent technical support during the cell culture work and Karin Landrock for the elemental analyses. This work was supported by the Helmholtz Initiative and Networking Fund (Functional nanomaterials for multimodality cancer imaging (NanoTracking), project ID: VH-VI-421) and the Australian Research Council through a Future Fellowship to B.G. (FT130100838) and a Discovery Outstanding Researcher Award and Discovery Grant to L.S. (DP130100816). Support by the Structural Characterization Facilities at the Ion Beam Center of the HZDR is gratefully acknowledged.

Keywords: iron oxide nanoparticles • zwitterionic coatings • protein corona • macrophages• proteomics

[1] D. Ling, T. Hyeon, *Small* **2013,** *9*, 1450.
[2] Z. Zhou, L. Wang, X. Chi, J. Bao, L. Yang, W. Zhao, Z. Chen, X. Wang, X. Chen, J. Gao, *ACS Nano* **2013,** *7*, 3287.
[3] K. P. García, K. Zarschler, L. Barbaro, J. A. Barreto, W. O'Malley, L. Spiccia, H. Stephan, B. Graham, *Small* **2014,** *10*, 2516.
[4] J. Nam, N. Won, J. Bang, H. Jin, J. Park, S. Jung, S. Jung, Y. Park, S. Kim, *Adv. Drug Deliv. Rev.* **2013,** *65*, 622.

[5] K. E. Sapsford, W. R. Algar, L. Berti, K. B. Gemmill, B. J. Casey, E. Oh, M. H. Stewart, I. L. Medintz, *Chem. Rev.* **2013,** *113*, 1904.

[6] J. Wang, J. D. Byrne, M. E. Napier, J. M. DeSimone, *Small* **2011,** *7*, 1919.

[7] J. Feng, H. Liu, K. K. Bhakoo, L. Lu, Z. Chen, *Biomaterials* **2011,** *32*, 6558.

[8] S. T. Kim, K. Saha, C. Kim, V. M. Rotello, *Acc. Chem. Res.* **2013,** *46*, 681.

[9] D. F. Moyano, M. Goldsmith, D. J. Solfiell, D. Landesman-Milo, O. R. Miranda, D. Peer, V. M. Rotello, *J. Am. Chem. Soc.* **2012,** *134*, 3965.

[10] H. S. Choi, W. Liu, P. Misra, E. Tanaka, J. P. Zimmer, B. Itty Ipe, M. G. Bawendi, J. V. Frangioni, *Nat. Biotechnol.* **2007,** *25*, 1165.

[11] C. D. Walkey, W. C. Chan, *Chem. Soc. Rev.* **2012,** *41*, 2780.

[12] M. P. Monopoli, C. Aberg, A. Salvati, K. A. Dawson, *Nat. Nanotechnol.* **2012,** *7*, 779.

[13] A. Salvati, A. S. Pitek, M. P. Monopoli, K. Prapainop, F. B. Bombelli, D. R. Hristov, P. M. Kelly, C. Aberg, E. Mahon, K. A. Dawson, *Nat. Nanotechnol.* **2013,** *8*, 137.

[14] B. Pelaz, G. Charron, C. Pfeiffer, Y. Zhao, J. M. de la Fuente, X. J. Liang, W. J. Parak, P. Del Pino, *Small* **2013,** *9*, 1573.

[15] M. Lundqvist, J. Stigler, T. Cedervall, T. Berggard, M. B. Flanagan, I. Lynch, G. Elia, K. Dawson, *ACS Nano* **2011,** *5*, 7503.

[16] K. Zarschler, L. Rocks, N. Licciardello, L. Boselli, E. Polo, K. P. Garcia, L. De Cola, H. Stephan, K. A. Dawson, *Nanomed. Nanotech. Biol. Med.* **2016**, *12*, 1663-1701.

[17] K. Knop, R. Hoogenboom, D. Fischer, U. S. Schubert, *Angew. Chem. Int. Ed.* **2010,** *49*, 6288.

[18] K. Viehweger, L. Barbaro, K. P. Garcia, T. Joshi, G. Geipel, J. Steinbach, H. Stephan, L. Spiccia, B. Graham, *Bioconjug. Chem.* **2014,** *25*, 1011.

[19] A. S. Karakoti, S. Das, S. Thevuthasan, S. Seal, *Angew. Chem.Int. Ed.* **2011,** *50*, 1980.

[20] Z. Estephan, P. Schlenoff, J. Schlenoff, *Langmuir* **2011,** *27*, 6794.

[21] J. Liu, M. Yu, X. Ning, C. Zhou, S. Yang, J. Zheng, *Angew. Chem Int. Ed.* **2013,** *52*, 12572.

[22] M. Ferriz-Manas, J. B. Schlenoff, *Langmuir* **2014,** *30*, 8776.

[23] D. F. Moyano, K. Saha, G. Prakash, B. Yan, H. Kong, M. Yazdani, V. M. Rotello, *ACS Nano* **2014,** *8*, 6748.

[24] K. Susumu, E. Oh, J. B. Delehanty, J. B. Blanco-Canosa, B. J. Johnson, V. Jain, W. J. t. Hervey, W. R. Algar, K. Boeneman, P. E. Dawson, I. L. Medintz, *J. Am. Chem. Soc.* **2011,** *133*, 9480.

[25] A. K. Murthy, R. J. Stover, W. G. Hardin, R. Schramm, G. D. Nie, S. Gourisankar, T. M. Truskett, K. V. Sokolov, K. P. Johnston, *J. Am. Chem. Soc.* **2013,** *135*, 7799.

[26] X. Wang, R. Wang, Y. Zheng, L. Sun, L. Yu, J. Jiao, R. Wang, *J. Phys. Chem. B* **2013,** *117*, 1886.

[27] H. Wei, O. T. Bruns, O. Chen, M. G. Bawendi, *Integr. Biol.* **2013,** *5*, 108.

[28] S. Mondini, M. Leonzino, C. Drago, A. M. Ferretti, S. Usseglio, D. Maggioni, P. Tornese, B. Chini, A. Ponti, *Langmuir* **2015,** *31*, 7381.

[29] Z. G. Estephan, H. H. Hariri, J. B. Schlenoff, *Langmuir* **2013,** *29*, 2572.

[30] D. Kim, M. K. Chae, H. J. Joo, I. H. Jeong, J. H. Cho, C. Lee, *Langmuir* **2012,** *28*, 9634.

[31] E. Giovanelli, E. Muro, G. Sitbon, M. Hanafi, T. Pons, B. Dubertret, N. Lequeux, *Langmuir* **2012,** *28*, 15177.

[32] X. Y. Sun, S. S. Yu, J. Q. Wan, K. Z. Chen, *J. Biomed. Mater. Res. A* **2013,** *101*, 607.

[33] W. Xiao, J. Lin, M. Li, Y. Ma, Y. Chen, C. Zhang, D. Li, H. Gu, *Contrast Media Mol. Imaging* **2012,** *7*, 320.

[34] L. Qi, X. Gao, *ACS Nano* **2008,** *2*, 1403.

[35] C. J. Huang, Y. Li, S. Jiang, *Anal. Chem.* **2012,** *84*, 3440.

[36] Y. Chang, S. Chen, Q. Yu, Z. Zhang, M. Bernards, S. Jiang, *Biomacromolecules* **2007,** *8*, 122.

[37] J. T. Kirk, N. D. Brault, T. Baehr-Jones, M. Hochberg, S. Jiang, D. M. Ratner, *Biosens. Bioelectron.* **2013,** *42*, 100.

[38] S. Jiang, K. Ishihara, S. Cooper, *J. Biomater. Sci. Polym. Ed.* **2014,** *25*, 1459.

[39] Z. Liu, Y. Peng, T. Wang, G. Yuan, Q. Zhang, J. Guo, Z. Jiang, *J. Sep. Sci.* **2013,** *36*, 262.

[40] R. Hu, G. Li, Y. Jiang, Y. Zhang, J. J. Zou, L. Wang, X. Zhang, *Langmuir* **2013,** *29*, 3773.

[41] K. Pombo-Garcia, K. Zarschler, J. A. Barreto, J. Hesse, L. Spiccia, B. Graham, H. Stephan, *RSC Adv.* **2013,** *3*, 22443.

[42] B. H. Kim, N. Lee, H. Kim, K. An, Y. I. Park, Y. Choi, K. Shin, Y. Lee, S. G. Kwon, H. B. Na, J. G. Park, T. Y. Ahn, Y. W. Kim, W. K. Moon, S. H. Choi, T. Hyeon, *J. Am. Chem. Soc.* **2011,** *133*, 12624.

[43] B. M. Gorzelle, A. K. Hoffman, M. H. Keyes, D. N. Gray, D. G. Ray, C. R. Sanders, *J. Am. Chem. Soc.* **2002,** *124*, 11594.

[44] U. Holzwarth, N. Gibson, *Nat. Nanotechnol.* **2011,** *6*, 534.

[45] D. R. Larson, W. R. Zipfel, R. M. Williams, S. W. Clark, M. P. Bruchez, F. W. Wise, W. W. Webb, *Science* **2003,** *300*, 1434.

[46] J. Seidel, V. T. Pinkrah, J. C. Mitchell, B. Z. Chowdhry, M. J. Snowden, *Thermochim. Acta* **2004,** *414*, 47.

[47] V. T. Pinkrah, M. J. Snowden, J. C. Mitchell, J. Seidel, B. Z. Chowdhry, G. R. Fern, *Langmuir* **2003,** *19*, 585.

[48] S. M. Henry, M. E. H. El-Sayed, C. M. Pirie, A. S. Hoffman, P. S. Stayton, *Biomacromolecules* **2006,** *7*, 2407.

[49] H. K. Hall, *J. Am. Chem. Soc.* **1957,** *79*, 5441.

[50] S. R. Saptarshi, A. Duschl, A. L. Lopata, *J Nanobiotechnology* **2013,** *11*, 26.

[51] W. Liu, J. Rose, S. Plantevin, M. Auffan, J. Y. Bottero, C. Vidaud, *Nanoscale* **2013,** *5*, 1658.

[52] Z. J. Deng, M. Liang, M. Monteiro, I. Toth, R. F. Minchin, *Nat. Nanotechnol.* **2011,** *6*, 39.

[53] H. Pan, M. Qin, W. Meng, Y. Cao, W. Wang, *Langmuir* **2012,** *28*, 12779.

[54] J. S. Gebauer, M. Malissek, S. Simon, S. K. Knauer, M. Maskos, R. H. Stauber, W. Peukert, L. Treuel, *Langmuir* **2012,** *28*, 9673.

[55] J. Wang, U. B. Jensen, G. V. Jensen, S. Shipovskov, V. S. Balakrishnan, D. Otzen, J. S. Pedersen, F. Besenbacher, D. S. Sutherland, *Nano Lett.* **2011,** *11*, 4985.

[56] J. E. Gagner, M. D. Lopez, J. S. Dordick, R. W. Siegel, *Biomaterials* **2011,** *32*, 7241.

[57] C. C. Fleischer, C. K. Payne, *J. Phys. Chem. B* **2014,** *118*, 14017.

[58] C. C. Fleischer, U. Kumar, C. K. Payne, Biomater. Sci. **2013,** *1*, 975.

[59] C. C. Fleischer, C. K. Payne, *Acc. Chem. Res.* **2014,** *47*, 2651.

[60] U. Sakulkhu, M. Mahmoudi, L. Maurizi, J. Salaklang, H. Hofmann, *Sci. Rep.* **2014,** *4*, 5020.

[61] M. P. Monopoli, D. Walczyk, A. Campbell, G. Elia, I. Lynch, F. B. Bombelli, K. A. Dawson, *J. Am. Chem. Soc.* **2011,** *133*, 2525.

[62] V. Nanjappa, J. K. Thomas, A. Marimuthu, B. Muthusamy, A. Radhakrishnan, R. Sharma, A. Ahmad Khan, L. Balakrishnan, N. A. Sahasrabuddhe, S. Kumar, B. N. Jhaveri, K. V. Sheth, R. Kumar Khatana, P. G. Shaw, S. M. Srikanth, P. P. Mathur, S. Shankar, D. Nagaraja, R. [[61] M. P. Monopoli, D. Walczyk, A. Campbell, G. Elia, I. Lynch, F. B. Bombelli, K. A. Dawson, *J. Am. Chem. Soc.* **2011,** *133*, 2525.

[62] V. Nanjappa, J. K. Thomas, A. Marimuthu, B. Muthusamy, A. Radhakrishnan, R. Sharma, A. Ahmad Khan, L. Balakrishnan, N. A. Sahasrabuddhe, S. Kumar, B. N. Jhaveri, K. V. Sheth, R. Kumar Khatana, P. G. Shaw, S. M. Srikanth, P. P. Mathur, S. Shankar, D. Nagaraja, R. Christopher, S. Mathivanan, R. Raju, R. Sirdeshmukh, A. Chatterjee, R. J. Simpson, H. C. Harsha, A. Pandey, T. S. Prasad, *Nucleic Acids Res.* **2014,** *42*, D959.

[63] D. Docter, U. Distler, W. Storck, J. Kuharev, D. Wunsch, A. Hahlbrock, S. K. Knauer, S. Tenzer, R. H. Stauber, *Nat. Protoc.* **2014,** *9*, 2030.

[64] S. Tenzer, D. Docter, J. Kuharev, A. Musyanovych, V. Fetz, R. Hecht, F. Schlenk, D. Fischer, K. Kiouptsi, C. Reinhardt, K. Landfester, H. Schild, M. Maskos, S. K. Knauer, R. H. Stauber, *Nat. Nanotech.* **2013,** *8*, 772.

[65] P. J. Boersema, R. Raijmakers, S. Lemeer, S. Mohammed, A. J. R. Heck, *Nat. Protoc.* **2009,** *4*, 484.

[66] Q. Dai, Y. Yan, C. S. Ang, K. Kempe, M. M. Kamphuis, S. J. Dodds, F. Caruso, *ACS Nano* **2015,** *9*, 2876.
[67] M. Pathan, S. Keerthikumar, C. S. Ang, L. Gangoda, C. Y. J. Quek, N. A. Williamson, D. Mouradov, O. M. Sieber, R. J. Simpson, A. Salim, A. Bacic, A. F. Hill, D. A. Stroud, M. T. Ryan, J. I. Agbinya, J. M. Mariadason, A. W. Burgess, S. Mathivanan, *Proteomics* **2015,** *15*, 2597.
[68] S. A. Love, M. A. Maurer-Jones, J. W. Thompson, Y. S. Lin, C. L. Haynes, *Annu. Rev. Anal. Chem.* **2012,** *5*, 181.
[69] B. J. Marquis, S. A. Love, K. L. Braun, C. L. Haynes, *Analyst* **2009,** *134*, 425.
[70] M. A. Dobrovolskaia, P. Aggarwal, J. B. Hall, S. E. McNeil, *Mol. Pharm.* **2008,** *5*, 487.
[71] K. Saha, D. F. Moyano, V. M. Rotello, *Mater. Horiz.* **2014,** *1*, 102.
[72] M. Elsabahy, K. L. Wooley, *Chem. Soc. Rev.* **2013,** *42*, 5552.
[73] Y. Yan, K. T. Gause, M. M. J. Kamphuis, C.-S. Ang, N. M. O'Brien-Simpson, J. C. Lenzo, E. C. Reynolds, E. C. Nice, F. Caruso, *ACS Nano* **2013,** *7*, 10960.
[74] D. Huhn, K. Kantner, C. Geidel, S. Brandholt, I. De Cock, S. J. Soenen, P. Rivera Gil, J. M. Montenegro, K. Braeckmans, K. Mullen, G. U. Nienhaus, M. Klapper, W. J. Parak, *ACS Nano* **2013,** *7*, 3253.
[75] A. Lesniak, F. Fenaroli, M. R. Monopoli, C. Aberg, K. A. Dawson, A. Salvati, *ACS Nano* **2012,** *6*, 5845.
[76] J. Park, K. An, Y. Hwang, J. G. Park, H. J. Noh, J. Y. Kim, J. H. Park, N. M. Hwang, T. Hyeon, *Nat. Mater.* **2004,** *3*, 891.
[77] K. A. Granath, *J. Colloid Interface Sci.* **1958,** *13*, 308.
[78] T. C. Laurent, K. A. Granath, *Biochim. Biophys. Acta* **1967,** *136*, 191.
[79] E. Dulkeith, M. Ringler, T. A. Klar, J. Feldmann, A. Munoz Javier, W. J. Parak, *Nano Lett.* **2005,** *5*, 585.
[80] A. J. Rai, C. A. Gelfand, B. C. Haywood, D. J. Warunek, J. Yi, M. D. Schuchard, R. J. Mehigh, S. L. Cockrill, G. B. Scott, H. Tammen, P. Schulz-Knappe, D. W. Speicher, F. Vitzthum, B. B. Haab, G. Siest, D. W. Chan, *Proteomics* **2005,** *5*, 3262.
[81] K. Zarschler, K. Prapainop, E. Mahon, L. Rocks, M. Bramini, P. M. Kelly, H. Stephan, K. A. Dawson, *Nanoscale* **2014,** *6*, 6046.
[82] K. Zarschler, S. Witecy, F. Kapplusch, C. Foerster, H. Stephan, *Microb. Cell Fact.* **2013,** *12*, 97.

Entry for the Table of Contents

FULL PAPER

Non-stick coating: Ultrasmall superparamagnetic iron oxide nanoparticles coated with a zwitterionic, amphiphilic polymer exhibit excellent colloidal stability, high resistance to protein corona formation, minimal cytotoxicity and very low levels of cellular uptake. Moreover, they do not elicit an inflammatory cytokine response or exhibit hemolytic activity *in vitro*, thereby representing a promising platform for development of "stealth" imaging/therapeutic agents.

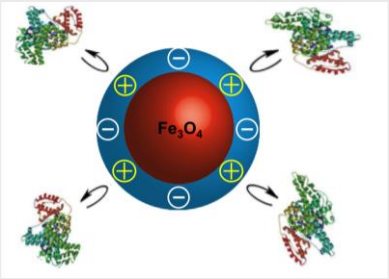

K. Pombo-García, S. Weiss, K. Zarschler, C.-S. Ang, R. Hübner, J. Pufe, S. Meister, J. Seidel, J. Pietzsch, L. Spiccia, H. Stephan,* B. Graham**

Page No. – Page No.

Zwitterionic polymer-coated ultrasmall superparamagnetic iron oxide nanoparticles with low protein interaction and high biocompatibility

Additional Author information for the electronic version of the article.

Bim Graham: orcid.org/0000-0002-1160-7751